

Robust eco-design: A new application for air quality engineering

IRAD BEN-GAL*, RONI KATZ and YOSSI BUKCHIN

Department of Industrial Engineering, Tel-Aviv University, Israel, 69778
E-mail: bengal@eng.tau.ac.il

Received July 2006 and accepted October 2007

The method of robust design has long been used for the design of systems that are insensitive to noises. In this paper it is demonstrated how this approach can be used to obtain a robust eco-design (ecological design). In a case study, robust design principles are applied to the design of a factory smokestack, using the Gaussian Plume Model (GPM). The GPM is a well-known model for describing pollutant dispersal from a point source, subject to various atmospheric conditions. In this research, the mean-square-error (MSE) of the accumulated and the maximum pollution values around a given target are defined as the performance measures and used to adjust the design parameters. Both analytical and numerical approaches are used to evaluate the MSE measures over the design space. It is demonstrated how to use the non-linearity in the GPM to reach a low MSE value that produces a cheaper design configuration. The differences between the manufacturer viewpoint and the environmentalist viewpoint with respect to the considered eco-design problem are discussed and analyzed.

Keywords: Ecological design, green manufacturing, air pollution, clean production

1. Introduction: Eco-design and quality engineering

The concept of *eco-design*, often referred to as *cleaner production* or *design for the environment*, describes a design process which takes into consideration the environmental implications of a designed product or process by using various approaches. The goal of such a process is to eliminate undesirable or potentially hazardous effects on the environment. The trend of cleaner production first emerged in the 1970s, owing to the growing understanding of the dangerous effects of pollution, which led to increasing pressure on governments and organizations to control and limit its spread. The early efforts to produce cleaner production focused on reducing the impact of pollution and waste *after* they have been produced, using “end of pipe” methods (Roy, 2000). However, since the late-1980s, attention has gradually shifted toward efforts to integrate environmental considerations into the planning and design phase—first to the production process and later to the products themselves. A similar trend was observed in the area of quality engineering, where efforts have shifted in the last decades from sampling and testing to robust design (Phadke, 1989; Kenett and Zacks, 1998).

Research has been focused on the end of the product’s life cycle. O’Brien (2002) addresses the sustainability of the design and manufacture of products, while presenting a closed-loop concept for industry, in which inputs of raw materials and return of waste to the environment must be minimized or eliminated. Nakashima *et al.* (2002) explicitly handle the product recovery system, in which parts and materials of the products are reused and recycled in order to minimize waste and environmental damage. To that end, some research has been conducted to address the disassembly process used for product recovery (see, e.g., Dini *et al.* (2001) and Guèngoè and Gupta (2002)).

There is a large body of research that deals with eco-design, which is associated with non-quantitative models and qualitative discussions. Shu-Yang *et al.* (2004) present seven principles of eco-design and conclude that any form of design that minimizes environmental impact by emulating and integrating with natural ecosystems can be referred to as eco-design. They also state that eco-design seeks to provide a framework for an environmentally appropriate system of design and management by incorporating both anthropogenic and ecological values, at relevant spatial and temporal scales (see, also, Todd and Todd (1994) and Scott (1999)).

Nissen (1995) gives a list of traits which characterize an *eco-product*—a product that already incorporates environmental considerations within its design : i) the material used

*Corresponding author

is a plentiful natural resource; ii) the manufacturing process requires only a low consumption of natural resources; iii) the emission of hazardous waste in the production process is minimal; iv) when in use, the product is relatively environmentally sound; v) environmentally sound remanufacturing or recycling processes can be easily applied after use; and vi) when finally discarded, the environmental impact of disposal/incineration is minimal.

In this paper, we suggest the implementation of an analytical approach, which may be most useful in achieving the third characteristics listed in Nissen (1995). The method is based on *quality engineering* concepts, and particularly on the approach of *robust design* which was originally proposed by Taguchi (1978) and later integrated with other “offline quality engineering” principles. The method aims to design products or processes which are robust, i.e., insensitive to the effects of noise sources as intended under a wide range of conditions. Some applications and discussions of the principles of robust design can be found in Fowlkes and Creveling (1995) and Kenett and Zacks (1998).

Although the statistical foundations of the Taguchi methods have been criticized over the years (e.g., Leon *et al.* (1987), Box (1988), and Steinberg and Burszty (1994)), the principles of robust design have been widely applied to diverse areas, such as the design of VLSIs, optimization of communication networks, development of electronic circuits, laser engraving of photo masks, cash-flow optimization in banking, government policy making, and runway utilization improvement at airports (Ross, 1988; Phadke, 1989; Rupe and Gavirneni, 1995; Taguchi, 1995).

In this paper we consider a robust eco-design of a system whose output (quality characteristic) is the pollution level emitted from its source. In particular, our analyzed case study deals with a robust design of a factory smokestack. The applied pollution model is the well-known *Gaussian Plume Model* (GPM) of pollution dispersal from a point source. Using robust design principles, one can divide the factors included in this model into controllable factors and noise factors. The *controllable factors* (called also the *design parameters*), such as the physical dimensions of the stack, are selected by the designer. The uncontrollable *noise factors* such as temperature, wind velocity and other atmospheric conditions, are the source of variability in the system.

A common practice in robust design methods is to evaluate different settings of the controllable factors via experimentation, while observing their interactions with the noise factors. The designer then picks a design configuration that yields a robust output, which in our case is a low and relatively constant pollution level under various atmospheric conditions. The output pollution level is characterized by its mean value and its variance. A low pollution value is often desirable; therefore one option is to use Taguchi’s “*the-smaller-the-better*” criterion, where the designer aims to minimize the system output, since quality decreases with the system output. However, note that in practice, most designers of polluting systems are highly committed to rev-

enues and cost–benefit considerations rather than a “zero-pollution” level. Total elimination of pollution is often too costly, unrealistic and, therefore, is not enforced by governmental regulations. Thus, another option is to use Taguchi’s *nominal-the-best* criterion, where the designer aims to set the output to a predefined target value. In this paper, we apply this criterion to the “required” pollution level. We find this criterion appealing since it enables us to analyze the robust eco-design from two conflicting viewpoints simultaneously—that of the “environmentalist”, aiming to reach a “zero” target for the pollution level, and that of the manufacturer, aiming to maintain a given pollution limit, as set by environmental regulations, while minimizing his/her costs. Given a target value, the designer aims to set the control factors such that the output mean value is adjusted to the target while minimizing the output variance (i.e., its sensitivity to noise). A widely used measure that takes into consideration shifts in both the output’s mean and its variance is the Mean-Square Error (MSE) measure. This measure enables analysis of the tradeoff between shifts in the output mean and the output variance that have an important practical implication in the case of eco-design as discussed below. We demonstrate how to implement a robust eco-design approach to obtain a desirable system configuration that yields a small MSE measure. We use two alternative approaches for computing the MSE measure. The first approach is analytic, based on expanding the pollution model to a Taylor series. The second approach is numeric, based on Monte Carlo simulations that estimate the MSE empirically.

The above analysis relies on the GPM transfer functions that express the effects of the control and the noise factors (as well as their interactions) on the MSE pollution level. Taguchi proposed to exploit the possible non-linearity in a model’s transfer functions in order to minimize the output variance, while fixing the mean value to a predetermined target (e.g., Phadke (1989)). We follow this idea, which is particularly appealing in the context of eco-design since most pollution models, including the GPM, rely on non-linear transfer functions.

2. Evaluating the MSE value for a given transfer function

We use the MSE of a random pollutant output y with respect to a prespecified target M as our performance measure. The MSE function is related to Taguchi’s *loss function* (Phadke, 1989) and depends on the output variance and mean values, that is

$$MSE(y) = V(y) + (E(y) - M)^2. \quad (1)$$

Given n observations of the pollutant output, the MSE value can be estimated as follows:

$$\begin{aligned} M\hat{S}E &= \frac{1}{n} \sum_{i=1}^n (y_i - M)^2 \\ &= \hat{\sigma}^2 + (\hat{\mu} - M)^2, \end{aligned}$$

where y_i is the i th observed output, $\hat{\sigma}^2$ is the output sample variance and $\hat{\mu}$ is the output sample mean. Two alternative approaches are used here to estimate the MSE measure, one analytical and the other numerical.

2.1. The analytical approach

The analytical approach is well illustrated in Kenett and Zacks (1998). It derives the loss function of the output y from its approximated mean and variance. In particular, it expands the input–output transfer function $y = f(\boldsymbol{\theta}, \mathbf{X})$, where $\boldsymbol{\theta}$ is a vector of control factors, and \mathbf{X} is a vector of k noise factors. Let the noise factors (X_1, X_2, \dots, X_k) have a respective vector of mean values $\boldsymbol{\xi} = (\xi_1, \xi_2, \dots, \xi_k)$ and a variance–covariance matrix as follows:

$$\mathbf{V} = \begin{bmatrix} \sigma_1^2 & \sigma_{12} & \cdots & \sigma_{1k} \\ \sigma_{21} & & & \\ \vdots & \ddots & & \vdots \\ \sigma_{k1} & \sigma_{k2} & & \sigma_k^2 \end{bmatrix}. \quad (2)$$

We assume that based on numerous past observations, both the mean values and the variance–covariance matrix values are known. Otherwise, we shall use their maximum likelihood estimates. Let us expand $f(\boldsymbol{\theta}, \mathbf{X})$ into a second-order Taylor series around $\boldsymbol{\xi}$ to obtain:

$$f(\boldsymbol{\theta}, \mathbf{X}) \cong f(\boldsymbol{\theta}, \boldsymbol{\xi}) + \sum_{i=1}^k (X_i - \xi_i) \frac{\partial}{\partial X_i} f(\boldsymbol{\theta}, \boldsymbol{\xi}) + \frac{1}{2} (\mathbf{X} - \boldsymbol{\xi})' \mathbf{H}(\boldsymbol{\theta}, \boldsymbol{\xi}) (\mathbf{X} - \boldsymbol{\xi}), \quad (3)$$

where $\mathbf{H}(\boldsymbol{\theta}, \boldsymbol{\xi})$ is the Hessian, a $k \times k$ matrix of second-order partial derivatives evaluated at $\boldsymbol{\xi}$, with the (i, j) th element equal to

$$H_{ij}(\boldsymbol{\theta}, \boldsymbol{\xi}) = \frac{\partial^2}{\partial X_i \partial X_j} f(\boldsymbol{\theta}, \boldsymbol{\xi}), \quad i, j = 1, 2, \dots, k. \quad (4)$$

Then, we obtain the following approximation for the function mean value:

$$E\{f(\boldsymbol{\theta}, \mathbf{X})\} \cong f(\boldsymbol{\theta}, \boldsymbol{\xi}) + \frac{1}{2} \sum_{i=1}^k \sum_{j=1}^k \sigma_{ij} H_{ij}(\boldsymbol{\theta}, \boldsymbol{\xi}), \quad (5)$$

and for its variance:

$$V\{f(\boldsymbol{\theta}, \mathbf{X})\} \cong \sum_{i=1}^k \sum_{j=1}^k \sigma_{ij} \frac{\partial}{\partial X_i} f(\boldsymbol{\theta}, \boldsymbol{\xi}) \frac{\partial}{\partial X_j} f(\boldsymbol{\theta}, \boldsymbol{\xi}). \quad (6)$$

Expressing the pollutant output by its transfer function $y = f(\boldsymbol{\theta}, \mathbf{X})$ and substituting Equations (5) and (6) into Equation (1), we obtain an analytical approximation for the MSE measure for various values of noise and control factors. Note that for non-linear transfer functions, both the expected value (5) and the variance (6) depend on the set of control and noise factors, as well as the noise factors variance–covariance matrix (2). Keeping in mind that

our goal is to minimize the MSE (with respect to the target M), which depends on Equations (5) and (6), we realize that for a non-linear transfer function we may obtain a “tradeoff” behavior. Namely, a specific set of parameters can minimize the bias component while maximizing the variance component or *vice versa*, as these components are not independent of each other. Since the functions describing pollution-related behaviors are often complex and non-linear, we expect to deal with such tradeoffs when applying the robust eco-design method. This phenomenon is further illustrated by two case studies in Section 4.

2.2. The numerical approach

The numerical approach for the evaluation of the MSE is based on a Monte Carlo simulation. Since the transfer functions are assumed to be known, it is possible to replicate random (weather) conditions for each set of the stack’s design parameters. Each replication yields a single realization of the system’s output under the considered design parameters. Given a sufficient number of such realizations, we can estimate the mean and the variance of the output empirically.

Note that both the analytical and the numerical approaches are complementary to each other. The analytical approximation enables analysis of a continuous design space, which is relatively large, with a low computational cost. The numerical approach, which is more costly in terms of computation time, can be used to validate the accuracy of the analytical approach at certain (discrete) design points. Both approaches are used in the case studies in Section 4.

3. The GPM

We analyze a classical air pollutant concentration model known as the GPM. We use the GPM to demonstrate the advantages in applying the robust eco-design method, albeit the method can be applied to numerous other pollutant dispersal models. In this section we briefly introduce the main transfer functions of the GPM. For a more detailed description, turn to De Nevers (1995), Heinsohn and Kabel (1999) and Pepper *et al.* (1996).

The GPM is a basic model dealing with *atmospheric diffusion* or *atmospheric dispersion*. In its typical form, it is used to describe the downwind concentrations of a pollutant, resulting from a point source such as a factory smokestack (a smokestack is not a “real” point source, but a small area that can be approximated as a point source). The pollutant stream exits a stack of geometric height h_s . It rises vertically a distance δh , called the *plume rise*, until the upward momentum and/or buoyancy ceases at the *effective stack height* $H = h_s + \delta h$, where it is transported downwind. Later it is seen that δh depends on the stack’s height and diameter. The common coordinate system used

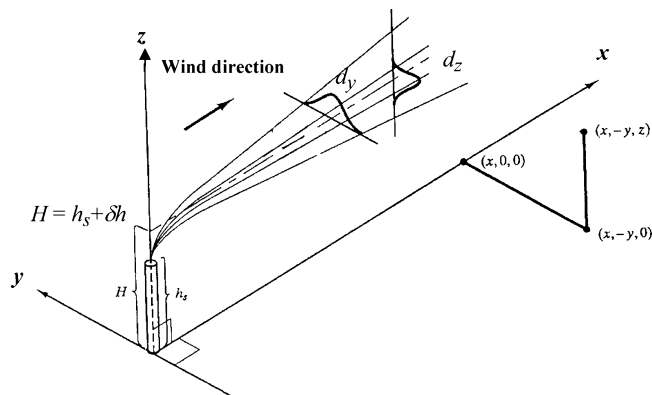


Fig. 1. Graphical illustration of the GPM.

to describe the pollutant's advance orients the x -axis in the direction of the prevailing wind, the z -axis vertically upward, and the y -axis transverse to the wind. The coordinates are all described with respect to the smokestack's base as seen in Fig. 1 (Heinsohn and Kabel, 1999).

The general GPM describes the concentration of the pollutant at any point of the plume. For simplicity, we limit our discussion to the pollutant's ground level concentration down the central line of the plume, which is calculated at some distance x downwind from the stack center:

$$c_i^{GL}(x, 0, 0) = \frac{\dot{m}_{i,s}}{U_H \pi d_y d_z} \exp \left[-\frac{1}{2} \left(\frac{H}{d_z} \right)^2 \right], \quad (7)$$

where, $\dot{m}_{i,s}$ is pollutant i emission rate from the stack (in kilograms per second [kg/s]) units; U_H is the wind speed in the x -direction at the effective¹ stack height H (in meters [m]); while d_y and d_z are the *dispersion coefficients* in the transverse (y) and vertical (z) directions respectively.

The values of d_y and d_z are evaluated empirically and depend on the stability condition, which refers to the ability of the system to return to its initial state after being perturbed from equilibrium. It is common to use the letters A to F to classify the basic stability conditions, where A, B and C refer to unstable conditions; D refers to the neutral condition; and E and F refer to stable conditions, which suppress vertical dispersion of pollutants (the interested reader is referred to Hanna *et al.* (1982) for further details). One set of empirical expressions for evaluating d_y and d_z for different stability levels and urban sites are presented in Table 1 (Heinsohn and Kabel, 1999).

Equation (7) is based on the value of the effective stack height $H = h_s + \delta h$. The plume rise, δh , which represents the height to which the plume rises before it loses its upward

¹A conservative approach suggests using the wind speed at physical stack height rather than effective stack height. We aim to analyze the proposed robust method in a less conservative case.

Table 1. Empirical dispersion coefficients for urban sites (Heinsohn and Kabel, 1999).

Stability letters	Stability	d_y (m)	d_z (m)
A–B	Unstable	$0.32x(1 + 0.0004x)^{-0.5}$	$0.24x(1 + 0.0001x)^{0.5}$
C	Unstable	$0.22x(1 + 0.0004x)^{-0.5}$	$0.20x$
D	Neutral	$0.16x(1 + 0.0004x)^{-0.5}$	$0.14x(1 + 0.0003x)^{-0.5}$
E–F	Stable	$0.11x(1 + 0.0004x)^{-0.5}$	$0.08x(1 + 0.0015x)^{-0.5}$

momentum or buoyancy, can be calculated by using the Briggs equation, as given by Heinsohn and Kabel (1999):

$$\delta h = \left(114 \cdot \left(1.58 - 41.4 \frac{\Delta\Theta}{\Delta z} \right) \left(\frac{g v_s D_s^2 (T_s - T_a)}{4 T_a} \right)^{1/3} \right) / U_s, \quad (8)$$

where U_s is the wind speed at the stack exit (stack's height); v_s is the gas velocity at stack exit; D_s is the inside diameter of the stack exit; $g = 9.8 \text{ m/s}^2$; T_s is the gas temperature at stack exit in absolute units of [kelvin]; T_a is the ambient temperature at stack exit [in kelvin]; $\Delta\Theta/\Delta z$ is the potential temperature gradient—a meteorological parameter that depends on atmospheric stability (and determined by the lapse rate). Thus, the pollutant behavior is largely influenced by the *atmospheric stability* class, a meteorological concept describing the vigor of vertical mixing. In a *stable atmosphere*, buoyancy returns a parcel of air to its original position after it has been displaced upward or downward in an adiabatic fashion. An *unstable atmosphere* is one in which buoyancy increases the displacement of the parcel of air that has moved in an adiabatic fashion. The different *constants* used in the model (d_y , d_z and $\Delta\Theta/\Delta z$) are chosen according to the atmospheric stability level. Finally, the value of the wind speed at different heights (U_H and U_s in Equations (7) and (8), respectively) can be evaluated via the power-law function (Hanna *et al.*, 1982)

$$U_z = U_{10} \left(\frac{z}{10} \right)^p \quad z \leq 200 \text{ m}, \quad (9)$$

where z is the height in meters; U_{10} is the observed wind speed at 10 m; while the value of p is taken from Table 2 (Heinsohn and Kabel, 1999).

Table 2. Power-law exponents for atmospheric stability categories (Heinsohn and Kabel, 1999).

Location	A	B	C	D	E	F
Urban (p)	0.15	0.15	0.20	0.25	0.30	0.30
Rural (p)	0.07	0.07	0.10	0.15	0.35	0.55

3.1. The applicability of the GPM for robust eco-design

Examining Equations (7) and (8) reveals that the pollutant concentration at ground level downwind from the stack is represented by non-linear transfer functions. These functions depend upon three types of factors that are classified here as follows:

1. *Weather conditions*: the ambient temperature (T_a) and the wind speed at 10 m (U_{10}) that allows computation of the wind speed at various heights (denoted by U_s and U_H in the model). We consider these as clearly uncontrollable noise factors. For simplicity of exposition, other variables that are affected by the weather conditions such as d_y , d_z and $\Delta\Theta/\Delta z$ are defined and fixed according to the selected atmospheric stability level.
2. *Stack design parameters*: the stack height (h_s) and the stack diameter (D_s). We consider these as pure design parameters, i.e., the controllable factors.
3. *Manufacturing process characteristics*: the i th pollutant emission rate from the stack ($\dot{m}_{i,s}$), the gas velocity (v_s) and the temperature (T_s) at the stack exit. All these factors depend on the manufacturing process and can be treated either as controllable factors, if the designer wishes to redesign the process, or as noise factors if they are assumed to be uncontrollable. For simplicity reasons, we consider the process as rigid and fix the values of these variables.

The definition of these classes shows that the GPM model is suitable for the application of robust design methods, as described by the following case studies.

4. Case studies: robust eco-design of a smokestack via the GPM

2 We now implement the robust design method for the factory smokestack. Our objective is to find a suitable design for a factory stack, which emits SO_2 as a result of coal burning. In particular, we aim to minimize some functions of the pollutant's ground level concentration directly downwind of the stack over a range of distances from the point source. The analysis is based on the non-linear transfer functions (7) and (8), while the MSE measure is approximated by using Equations (5) and (6) or estimated numerically. For simplification purposes, we reduce the number of "free" parameters to four, considering two control factors and two noise factors. The control factors are the *stack diameter* (D_s), for which the feasible range is [1.8, 2.8] m, and the *stack physical height* (h_s), for which the feasible range is [50 m, 150 m]. These ranges are selected to illustrate the non-linearity effects of the control factors on the eco-robust solution as shown below. The two independent noise sources are the *wind speed* at 10 m (U_{10}) and the *ambient tempera-*

ture at stack exit (T_a) that are represented by known random variables. The first variable is assumed to follow a normal distribution with a mean of two and standard deviation 0.2, i.e., $U_{10} \sim N(2, 0.2)$ m/s. The second variable is assumed to follow a uniform distribution between 283–295 K, i.e., $T_a \sim U(283, 295)$ K. The distributions' mean values follow the examples given in Heinsohn and Kabel (1999) (see Sections 9.9 and 9.10). Our selection of these types of distributions is for illustration purpose. It does not affect the non-linearity behavior of the transfer function nor its applicability to robust eco-design, which is the main subject of this study. The rest of the parameters in the following case studies are based on the same examples from Heinsohn and Kabel (1999).

The two system outputs (that are considered in two different case studies) are y_{cum} , the *cumulative ground level concentration* of the pollutant over a discrete range of 1–10 km from the stack, and y_{max} the *maximum ground level concentration* of the pollutant over the same range. These outputs are defined here as follows:

$$y_{\text{cum}} = \sum_{x=1}^{10} c_i^{\text{GL}}(x, 0, 0) \text{ and}$$

$$y_{\text{max}} = \max_{x=1,2,\dots,10} c_i^{\text{GL}}(x, 0, 0) = c_i^{\text{GL}}(x_{\text{max}}, 0, 0). \quad (10)$$

Thus, y_{cum} is approximated by summing the pollutants concentration over ten discrete points from 1 to 10 km, while y_{max} is found over the same discrete points (starting the range from 0 km has a negligible effect on the outputs in our case study, since the location of the maximum ground level concentration in this case is above 1 km—mostly in the range of 5–8 km). Note that the cumulative ground level pollutant concentration, which gained some attention in recent years (e.g., Hunter (1999) and Daggubati *et al.* (2007)), can serve as a measure when considering the overall hazardous effects of a pollutant dispersal source. The use of a cumulative concentration measure can reveal a realistic situation where a point source causes significant environmental damage by the cumulative amount of pollutants it emits, although the *maximum ground level concentration* is relatively low due to stable weather conditions. Usually, however, the cumulative ground level concentration is not used for the evaluation of air pollutant health impacts. For this reason, in Section 4.4 we include another example with respect to the *maximum ground level concentration*, which is a standard output measure for reporting dispersion modeling results. In the first example we consider stable weather conditions (category F in Table 2) whereas in the second example we consider unstable weather conditions (category A). This is done to show that the proposed eco-design method can be developed for different measures and different weather conditions. Recall that for both considered output measures, our objective is to minimize the MSE measure (as reflected in Equation (1)) with respect to the target M being set either

close to zero (“environmentalist” viewpoint) or to some regulated level (“manufacturer” viewpoint). In Sections 4.1 to 4.3 we analyze the system from an “environmentalist” viewpoint with $M = 0$. Sections 4.4 and 4.5 also consider other values for M . Both examples highlight the potential implications of robust eco-design that rely on the obtained non-linear transfer functions and the clear tradeoff between the variance and the bias components in the MSE function.

4.1. Initial analysis for the cumulative ground level concentration

In this example, we consider the *cumulative ground level concentration* y_{cum} in urban settings with stable atmospheric conditions (category F in Table 1). The pollutant emission rate is $\dot{m}_{i,s} = 153,700 \text{ mg/s} = 58,836,360 \text{ ppb}$, the lapse rate is 4 K/Km , yielding $\Delta\Theta/\Delta z = 0.0058 \text{ K/m}$, $T_s = 400 \text{ K}$ and $v_s = 14.5 \text{ m/s}$.

Our initial analysis is based on a simple factorial experiment of the two design factors. For each factor we define three equally spaced levels within the design range, resulting in the following $3^2 = 9$ factorial experiment: $\{h_s, D_s\} = \{(150, 2.8), (100, 2.8), (50, 2.8), (150, 2.3), (100, 2.3), (50, 2.3), (150, 1.8), (100, 1.8), (50, 1.8)\}$, as seen in Tables 3 and 4. The output’s mean, variance and MSE (with respect to $M = 0$) are evaluated for each of the nine combinations of the design factors by both the analytical and the numerical approaches. Namely, the analytical approach applies Equations (7) to (10) to derive $y_{\text{cum}}(h_s, D_s, U_{10}, T_a)$ —a closed-form transfer function for the system output y_{cum} . It then generates the approximations for the output’s mean and its variance— $E\{y_{\text{cum}}\}$ and $V\{y_{\text{cum}}\}$ as in Equations (5) and (6). These expressions are simplified due to the assumed

Table 3. Analytical approach results for stable atmospheric conditions (category F).

D_s	h_s		
	150	100	50
2.8			
Run	1	2	3
Average	42.62	60.32	62.59
Var	38.31	105.78	209.216
MSE	1854.94	3744.44	4126.15
2.3			
Run	4	5	6
Average	57.14	83.33	92.82
Var	40.33	123.32	295.26
MSE	3305.66	7067.58	8910.08
1.8			
Run	7	8	9
Average	77.96	117.46	141.03
Var	35.43	125.61	383.96
MSE	6113.97	13923.4	20274.9

Table 4. Numerical approach results for stable atmospheric conditions (category F).

D_s	h_s		
	150	100	50
2.8			
Run	1	2	3
Average	42.4	60.13	62.67
Var	39.95	103.56	197.85
MSE	1838.09	3719.87	4124.93
2.3			
Run	4	5	6
Average	56.87	83.72	92.21
Var	42.17	120.16	288.11
MSE	3276.4	7130.1	8790.63
1.8			
Run	7	8	9
Average	77.92	117.74	141.9
Var	39.17	139.29	409.65
MSE	6111.35	14001.3	20546.62

independence of the noise factors:

$$\begin{aligned}
 & E\{y_{\text{cum}}(h_s, D_s, U_{10}, T_a)\} \\
 & \cong y_{\text{cum}}(h_s, D_s, \mu_{U_{10}}, \mu_{T_a}) \\
 & + \frac{1}{2} \left(\sigma_{U_{10}}^2 \times \frac{\partial^2 y_{\text{cum}}(\cdot)}{\partial U_{10}^2} + \sigma_{T_a}^2 \times \frac{\partial^2 y_{\text{cum}}(\cdot)}{\partial T_a^2} \right) \\
 & V\{y_{\text{cum}}(h_s, D_s, U_{10}, T_a)\} \\
 & \cong \sigma_{U_{10}}^2 \times \left(\frac{\partial y_{\text{cum}}(\cdot)}{\partial U_{10}} \right)^2 + \sigma_{T_a}^2 \times \left(\frac{\partial y_{\text{cum}}(\cdot)}{\partial T_a} \right)^2 \quad (11)
 \end{aligned}$$

The outputs of the analytical approach in the initial experiment are shown in Table 3.

The numerical approach uses the inverse transform method for both the Gaussian and the Uniform random variables to generate 1000 realizations of U_{10} and T_a for each of the examined design configurations. A simple way to generate these values is by using the inverse distribution functions in Excel. Thus, the generated values are based on a random sampling from the assumed distributions of the noise factors. Finally, using these realizations, $E\{y_{\text{cum}}\}$, $V\{y_{\text{cum}}\}$ and $MSE\{y_{\text{cum}}\}$ are estimated empirically. The results of the numerical approach in the initial experiment are given in Table 4.

Note that the mean values derived by both approaches are similar, ensuring that the analytical approximation is close enough to the “real/simulated” value. As for the MSE, the values of both approaches are convincingly close, although not identical, mainly due to the differences in the variance estimates. The variances are relatively high due to the stable atmospheric conditions, under which the pollution can be carried far away from the stack. Unintuitively, these variances decrease dramatically for the unstable atmospheric conditions (this analysis is not presented here)

when air turbulence pushes the pollutant to the ground level close to the stack exit.

At first sight, the results in Tables 3 and 4 seem quite trivial. The minimal accumulated pollution level and the lowest value of MSE is obtained for the highest and widest stack (run no. 1), which is not surprisingly the most expensive design configuration. A closer look at the results, however, reveals some inconsistencies resulting from the interactions between the factors. For example, while for a fixed 50 m stack height the variance clearly decreases in the stack diameter, for a fixed 150 m stack height the variance is non-monotonic in the stack diameter. That is, for the latter case the variance increases (e.g., in Table 3 from 35.43 to 40.33) when increasing the diameter (from 1.8 m to 2.3 m) but then surprisingly changes direction and decreases (e.g., in Table 3 from 40.33 to 38.31) with the second increase of the diameter (from 2.3 m to 2.8 m). For a 150 m stack height, the lowest variance value is obtained for $D_s = 1.8$ m and not, as expected, for $D_s = 2.8$ m. Similar interaction effects to those shown in Tables 3 and 4 are observed in Fig. 2, which depicts the MSE as a function of the stack height for different (fixed) stack diameters.

4.2. Analyzing a continuous design range

In this stage a more thorough investigation of the output’s mean, variance and MSE behavior is conducted based on the analytical approach for a continuous range of design space. We use *Mathematica* © software to draw these measures in Fig. 3. The figure shows the non-linear behavior of the mean (Fig. 3(a)), the variance (Fig. 3(b)) and the MSE with $M = 0$ (Fig. 3(c)) as a function of the design parameters. As can be seen, the MSE is mostly influenced by the output’s mean value, which is relatively high with respect to the output’s standard deviation.

The most practical observation from these figures is that the MSE behavior is, indeed, non-monotonous (i.e., shows a change of trend) in stack height for any fixed diameter at the considered ranges. Thus, given a fixed diameter, it

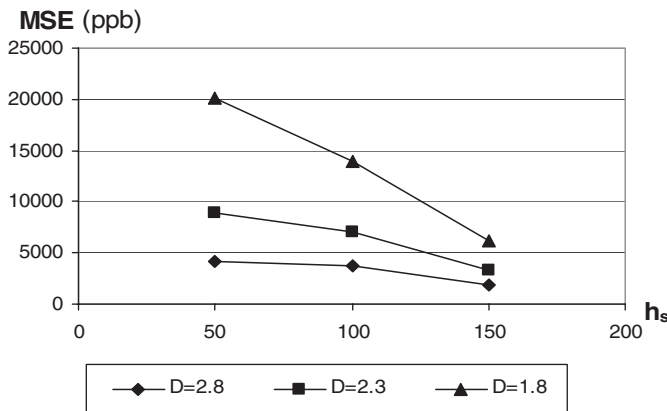


Fig. 2. MSE as a function of the stack height for different (fixed) stack diameters.

Table 5. “Zoom-in” analytical results for stable atmospheric conditions.

D_s	h_s		
	70	60	50
2.6			
Mean	77.92	75.69	73.10
Var	192.15	219.65	241.81
MSE	6263.01	5948.05	5585.58
2.4			
Mean	87.61	87.93	85.64
Var	211.86	246.42	276.98
MSE	7888.15	7977.63	7611.44
2.2			
Mean	101.45	102.50	100.69
Var	230.38	273.02	313.77
MSE	10522.08	10778.45	10451.85

is possible to obtain the same MSE values for both lower and higher stacks. The white dotted line in Fig. 3(c) for $D_s = 2.45$ m illustrates this phenomena—a similar MSE value can be obtained for low values of h_s (under 55 m) as well as for higher values (over 80 m). Since higher stacks are practically more expensive, this result implies that a cheaper solution may be found to the stack design problem, which is of equal quality with respect to the accumulated MSE measure.

4.3. “Zoom-in” analysis

We finalize our analysis by zooming into a smaller design region defined by the following parameters range: $h_s = [50, 70]$ m and $D_s = [2.2, 2.6]$ m. Once again, nine combinations of design parameters are defined based on an equally spaced factorial design: $\{h_s, D_s\} = \{(70, 2.6), (60, 2.6), (50, 2.6), (70, 2.4), (60, 2.4), (50, 2.4), (70, 2.2), (60, 2.2), (50, 2.2)\}$. The analytical and the numerical results are given in Tables 5 and 6, respectively.

Table 6. “Zoom-in” numerical results for stable atmospheric conditions based on 1000 replications.

D_s	h_s		
	70	60	50
2.6			
Mean	77.50	75.40	73.12
Var	180.39	199.82	229.18
MSE	6187.07	5885.18	5575.07
2.4			
Mean	88.16	88.34	85.18
Var	223.82	243.99	271.85
MSE	7996.43	8048.81	7527.40
2.2			
Mean	101.21	102.65	100.62
Var	236.75	274.20	300.15
MSE	10481.07	10810.57	10425.25

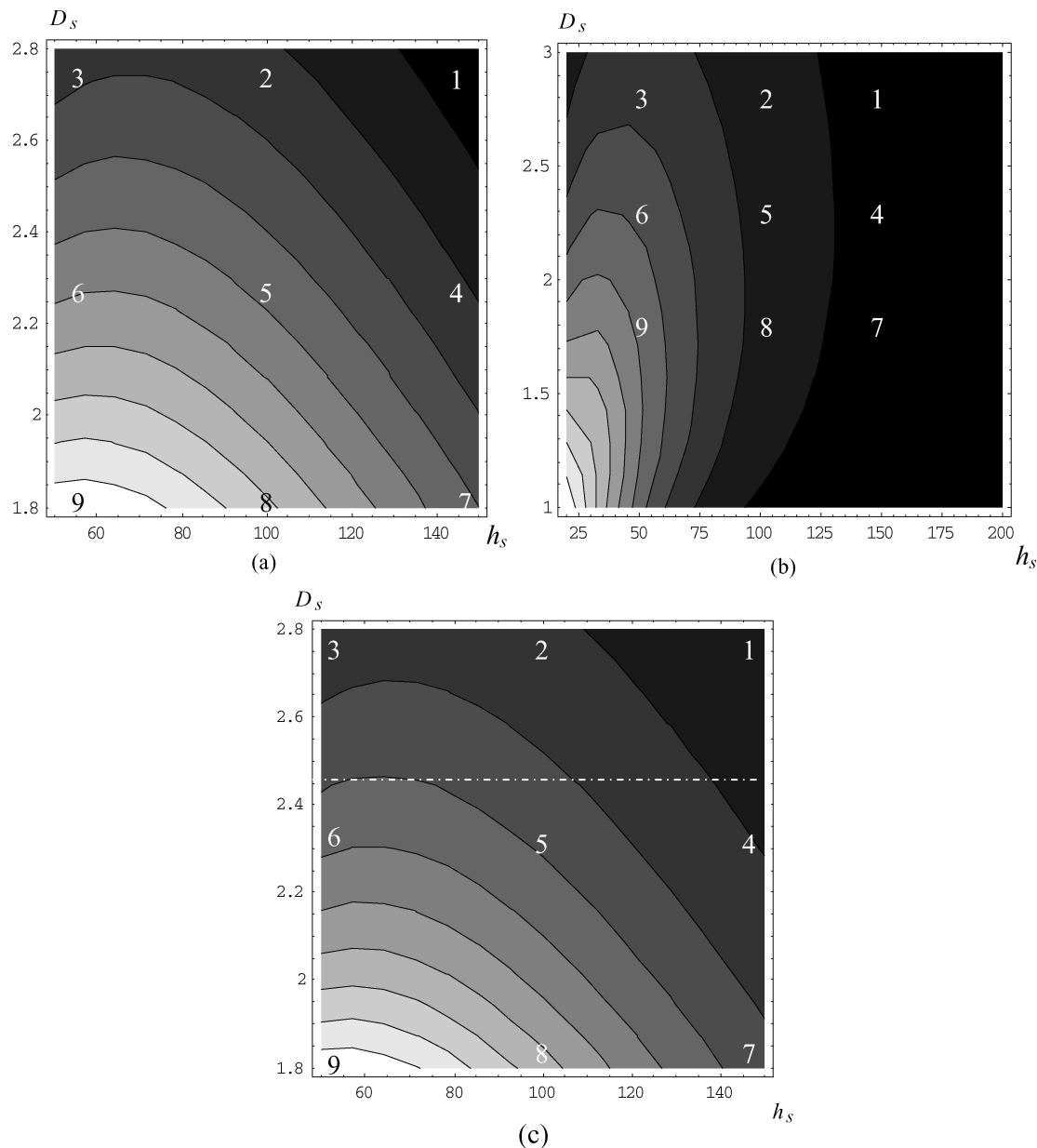


Fig. 3. (a) The output's mean; (b) variance; and (c) MSE as a function of the stack's height (h_s) and diameter (D_s). Lighter areas represent higher values. The numbers represent the nine discrete points that were investigated in the initial design (Tables 3 and 4).

These results strengthen our previous observations. For each of the suggested diameter values and for both analysis approaches, the obtained MSE for a stack height of 50 m is smaller and, therefore, better than those designs obtained for higher stacks.

The practical implication for an engineer dealing with the robust eco-design of the stack problem is that a better solution exists, which is a cheaper one with respect to the used MSE measure and the considered design range.

4.4. The maximum ground level concentration

As indicated above, the accumulative ground level concentration is not a standard measure in evaluating air pollu-

tant health impact. A commonly used measure is the *maximum ground level pollutant concentration*, as indicated by the National Ambient Air Quality Standards (NAAQS,² Chapter 3). Engineers are required to know the maximum ground level pollutant concentration, $c_i^{GL}(x_{\max}, 0, 0)$, for a particular stack's parameters and emission rates, and where this maximum value occurs. This location, downwind distance is denoted by x_{\max} , that is, the location where the ground level pollutant concentration achieves its maximum (see Equation (10)).

²See <http://www.epa.gov/air/criteria.html>

In this subsection we show that the same type of analysis regarding the applicability of robust eco-design applies also to the maximum ground level measure. This fact should not be surprising, since similar types of non-linear functions result from both measures.

Let us follow Heinsohn and Kabel (1999) for simplicity reasons and assume that the ratio of dispersion coefficients is a constant for any stability category, namely, $d_y/d_z = C$. Equation (7) can now be rewritten as

$$\frac{c_i^{GL}(x, 0, 0)U}{\dot{m}_{i,s}} = \frac{1}{\pi C d_z^2} \exp\left[-\frac{1}{2}\left(\frac{H}{d_z}\right)^2\right]. \quad (12)$$

Differentiating Equation (12) with respect to d_z and equating it to zero results in the optimal value of the dispersion coefficient $d_z^* = H/\sqrt{2}$. Plugging d_z^* into Equation (12) leads to the maximum normalized ground level concentration of unabsorbed gaseous pollutants:

$$\begin{aligned} \tilde{y}_{\max} &= \frac{c_i^{GL}(x_{\max}, 0, 0)U}{\dot{m}_{i,s}} = \frac{0.1171}{(H/\sqrt{2})^2} \\ &= \frac{0.2342}{(h_s + \delta h)^2}. \end{aligned} \quad (13)$$

Note that one can use Table 1 to find where x_{\max} is located by substituting the expressions for the dispersion coefficients as functions of x . Recall that δh is evaluated by using Equations (8) and (9). Evidently, Equation (13) is non-linear in the design and the noise factors and for $C = 1$ can be explicitly written as

$$\tilde{y}_{\max} = 0.2342 \times \left(h_s + \frac{114 \times (1.58 - 41.4(\Delta\Theta/\Delta z) \times (g v_s D_s^2 (T_s - T_a)/4T_a)^{1/3})^{-2}}{U_{10}(s/10)^p} \right)^{-2} \quad (14)$$

One can approximate both the expected value (by Equation (5)) and the variance (by Equation (6)) of the above function, and use them (by Equation (1)) to derive an approximation of $MSE(\tilde{y}_{\max})$. Since the goal is to minimize the MSE value with respect to some target, we expect a ‘‘tradeoff’’ behavior between the bias and the variance components. For illustration purpose, Fig. 4 plots the approximate $MSE(\tilde{y}_{\max})$ as a function of both the stack height h_s (between 10 and 220 m) and the target values (in the vicinity of $M = 0$) for a fixed diameter $D_s = 2.8$ m. Other parameters are set according to examples given in Section 9.7 in Heinsohn and Kabel (1999) for urban unstable conditions (category A in Table 1 with $p = 0.15$), where the lapse rate is 20 K/Km, resulting in $\Delta\Theta/\Delta z = -0.0102$ K/m, $T_a = 289$ K, $T_s = 450$ K and $v_s = 14.5$ m/s. Figure 4 reflects well the highly non-linear behavior that results from the inherent trade off within the MSE function. Moreover, it is seen that the MSE is highly sensitive to the target value in the vicinity of zero.

Finally, Table 7 shows a numerical analysis of the non-normalized measure $MSE(y_{\max})$ (see Equation (10)) for

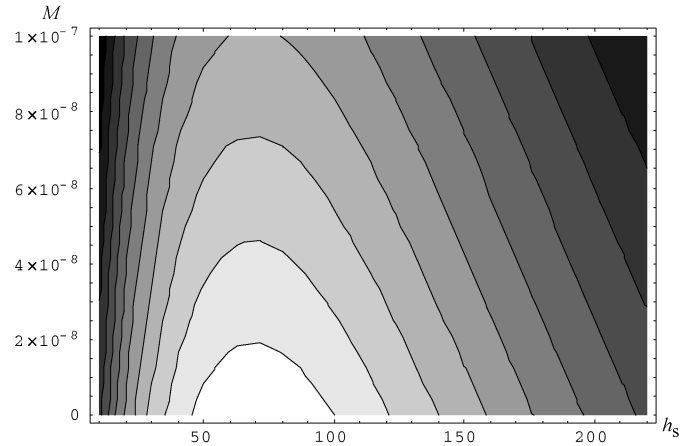


Fig. 4. The $MSE(\tilde{y}_{\max})$ contour plot as a function of both the stack height h_s and the target value M in the vicinity of zero. The stack’s diameter is fixed at $D_s = 2.8$ m.

an emission rate of $\dot{m}_{i,s} = 153,700$ mg/s = 58,836,360 ppb, as a function of the combinations of three values for the stack height $h_s \in 50$ m, 75 m and 100 m and three values for the stack diameter $D_s \in 2.6$ m, 2.7m and 2.8 m. Two different target values are considered here ($M = 12$ and $M = 8$). Other parameters are set according to the same examples given in Heinsohn and Kabel (1999).

Here again, the non-linear behavior of the MSE with respect to the stack height is evident. Note that for any fixed diameter value and for both target values, the MSE

Table 7. Numerical evaluation of $MSE(y_{\max})$ based on 1000 replications, as a function of the design parameters for unstable atmospheric conditions with respect to two different target values.

D_s	h_s		
	100	75	50
2.8			
Run no.	1	2	3
Avg	13.52	13.86	13.67
Var	0.67	0.86	1.05
MSE ($M = 12$)	2.98	4.31	3.83
MSE ($M = 8$)	31.12	35.16	33.19
2.7			
Run no.	4	5	6
Avg	14.00	14.40	14.24
Var	0.66	0.87	1.15
MSE ($M = 12$)	4.67	6.63	6.17
MSE ($M = 8$)	36.68	41.84	40.10
2.6			
Run no.	7	8	9
Avg	14.64	14.92	14.79
Var	0.70	1.00	1.27
MSE ($M = 12$)	7.68	9.52	9.03
MSE ($M = 8$)	44.81	48.87	47.31

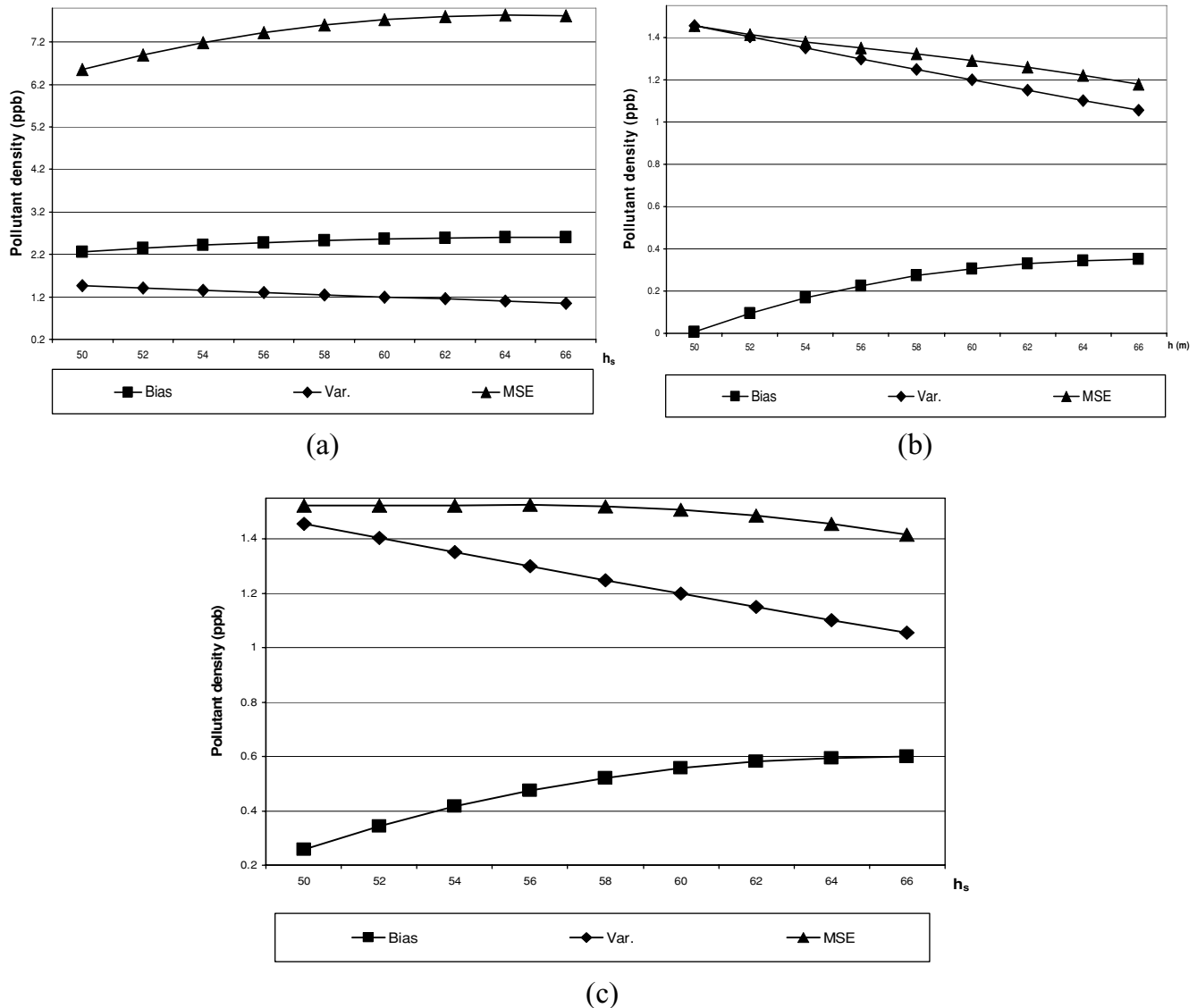


Fig. 5. The output bias, variance and MSE as a function of the stack height (50–66 m) for a fixed stack diameter of 2.6 m: (a) the regulated threshold is equal to 46 ppb; (b) the regulated threshold is equal to 48.5 ppb; (c) the regulated threshold is equal to 48 ppb.

value for the 50 m stack's height is lower than the MSE value for the 75 m stack's height. Thus, for a given diameter, the "cheaper" stack obtains better MSE values.

4.5. Robust design from the manufacturer's point of view

Thus far, we have applied the robust design method mainly from the "environmentalist's" point of view, trying to achieve a zero pollution level (with the exception of Table 7). However, in practice, the manufacturer, who has to comply with environmental regulations—often a given threshold set by the regulators—is usually interested in achieving an optimal design for a target function of the "nominal the best" type, as shown in Equation (1).

To illustrate such a case, we consider an example in which a designer is looking for the best height given a stack diam-

eter of 2.6 m, and under a given regulation for maximum allowed pollution level. We use the same performance measure as in Section 4.1, namely, the MSE of the cumulative pollutant concentration on the ground level with respect to the required regulation. Feasible heights ranging from 50 m to 66 m are examined. Both the output mean and the output variance are calculated, using the analytical approach. Finally, the MSE is computed with the given threshold as the target. The results are presented in Fig. 5.

A short review of these graphs leads to an interesting observation. For the diameter and height range in question, the bias component of the output Y (which depends on its mean value) increases in the stack height, whereas the variance component decreases in the stack height. When the target is equal to 46 ppb, the bias component is the dominating one on the MSE measure, i.e., the MSE increases

in h_s , (making lower values of h_s the better design choice). When the target is equal to 48.5 ppb, the variance becomes the dominating component on the MSE measure, which decreases in h_s (making higher values of h_s the better design choice). However, when the target is exactly 48 ppb, there is more of a balance between the two components of the MSE. Due to the non-linear transfer function, a tradeoff between the output mean and the output variance yields an almost constant MSE level for a significant range of heights. This phenomena in this case allows the designer to pick the most suitable design free of the MSE considerations. The selection between the two components of the MSE measure has also an important practical implication in the area of eco-design. Namely, from pollution prevention ("end of pipe") considerations (such as filtering devices etc.), it is often better to obtain a stabilized system with a slightly higher mean pollution value (reflected in a higher bias term) but a lower variance value. This phenomenon is even more significant if the regulated penalties on the pollution levels are proportional to their deviation from the threshold.

5. Conclusions and summary

In this paper we suggested applying concepts from robust design to systems with environmental and ecological implications. Eco-design, which is closely associated with emerging research areas such as *green manufacturing* and *sustainable design*, provides new and wide ranging applications to quality engineers. Using a particular case study, we showed that concepts of robust design and the Taguchi method are suitable for an eco-design that minimizes the emission of air pollutants and guarantees an environmentally sound use of a system.

Our case study focused on the design of a factory stack, aiming to obtain a stack that guarantees a minimal yet a stable cumulative pollutant concentration at ground level. To demonstrate the benefits in the suggested method, we used a combination of analytical and numerical analyses. We found some interesting phenomena that resulted from the non-linear transfer function of the GPM.

1. When considering the stack design from an environmentalist's viewpoint, aspiring to minimize the pollution level, one is able to take advantage of the non-linearity in the system output to choose a less expensive design of an equal air quality level.
2. When considering the viewpoint of the manufacturer, aiming to comply with given pollution regulations, one can directly deal with the tradeoff between the pollution variance and the bias components. This tradeoff allows the designer to pick a design from a wide range of solutions while carefully evaluating the effects of these two components.

Further investigations of the plume model may include the extension of the study to a thorough design of experiment analysis, while adding more design factors and investigating their joint effects simultaneously. Another potential direction is to relax some of the assumptions used in this paper, such as the independence between the various atmospheric conditions. All these extensions will potentially add to the non-linearity of model and, hence, provide further opportunities to exploit these non-linearities as suggested by Taguchi (1995). Finally, one can consider other applications of the robust design method to the field of eco-design, which contains numerous descriptive models that are analytically convenient.

References

- Box, G. (1988) Signal-to-noise ratios, performance criteria and transformation. *Technometrics*, **30**(1), 1–17.
- Daggbati, S.M., Benic, C.M. and Cheng, P. (2007) *Air Pollution Modeling and Its Application XVII*, Springer, New York.
- De Nevers, N. (1995) *Air Pollution Control Engineering*, McGraw-Hill, New York, NY, Chapters 5 and 6.
- Dini, G., Failli, F. and Santochi, M. (2001) A disassembly planning software system for the optimization of recycling processes. *Production Planning & Control*, **12**(1), 2–12.
- Fowlkes, W.Y. and Creveling, C.M. (1995) *Engineering Methods for Robust Product Design*, Addison-Wesley, Reading, MA.
- Guèngoèr, A. and Gupta, S.M. (2002) Disassembly line in product recovery. *International Journal of Production Research*, **40**(11), 2569–2589.
- Hanna, S.R., Briggs, G.A. and Hosker, R.P. Jr. (1982) *Handbook on Atmospheric Diffusion*, DOE/TIC-11223, (DE82002045) U.S. Dept. of Energy, Oak Ridge, TN.
- Heinsohn, R.J. and Kabel, R.L. (1999) *Sources and Control of Air Pollution*, Prentice Hall, Upper Saddle River, NJ, chapter 9.
- Hunter, C.H. (1999) Non-radiological air quality modeling for the high-level waste salt disposition, DOE Contract No. DE-AC09-96SR18500, WSRC-TR-99-00403, available at <http://www.osti.gov/bridge/purl.cover.jsp?purl=/15028-YHUra/webviewable/> accessed July 2008.
- Kenett, R.S. and Zacks, S. (1998) *Modern Industrial Statistics*, Brooks/Cole, Pacific Grove, CA, chapter 13.
- Leon, R.V., Shoemaker, A.C. and Kacker, R.N. (1987). Performance measures independent of adjustment. *Technometrics*, **29**(1), 253–285.
- Nakashima, K., Arimitsu, H., Nose, T. and Kuriyama, S. (2002) Analysis of a product recovery system. *International Journal of Production Research*, **40**(15), 3849–3856.
- Nissen, U. (1995) A methodology for the development of cleaner products. *Journal of Cleaner Production*, **3**(1/2), 83.
- O'Brien, C. (2002) Global manufacturing and the sustainable economy. *International Journal of Production Research*, **40**(15), 3867–3877.
- Pepper, I.L., Gerba, C.P. and Brusseau, M.L. (eds) (1996) *Pollution Science*, Academic Press, San Diego, CA.
- Phadke, M.S. (1989) *Quality Engineering using Robust Design*, Prentice Hall, Englewood Cliffs, NJ.
- Ross, P.J. (1988) *Taguchi Techniques for Quality Engineering*, McGraw-Hill, New York, NY.
- Roy, R. (2000) Sustainable product-service systems. *Futures*, **32**, 289–290.
- Rupe, A. and Gavirneni, S. (1995) Designing for high performance of a command, control, communication and information network. *IEEE Transactions on Reliability*, **44**, 230–236.
- Scott, F.A. (1999), *Ecological Design Handbook: Sustainable Strategies for Architecture, Landscape Architecture, Interior Design and Planning*. Donnelley & Sons, New York, NY

- Shu-Yang, F., Freedman, B. and Cote, R. (2004) Principles and practice of ecological design. *Environmental Reviews*, **12**(2), 97–112.
- Steinberg, D.M. and Bursztyn, D. (1994) Dispersion effects in robust-design experiments with noise factors. *Journal of Quality Technology*, **26**(1), 12–20.
- Taguchi G. (1978) Off-line and on-line quality control systems, in *Proceedings of the International Conference on Quality Control B4*, pp 1–5, Tokyo, Japan.
- Taguchi, G. (1995) Quality engineering (Taguchi methods) for the development of electronic circuit technology. *IEEE Transactions on Reliability*, **44**, 225–229.
- Todd, N.J. and Todd, J. (1994) *From Eco-Cities to Living Machines: Principles of Ecological Design* North Atlantic Books, Berkeley, CA.
- of *Statistical Planning and Inference*, as well as *Bioinformatics and BMC Bioinformatics*. He has received several research grants, from organizations such as General Motors, IEEE, the Israeli Ministry of Science, and the European Community. He has worked for several years in industrial organizations. His research interests include statistical methods for control and analysis of stochastic processes; applications of information theory to industrial problems; machine learning and automation and computer integrated manufacturing systems.
- Roni Katz is an Industrial Engineer. She holds a B.Sc. degree (2003) in Industrial Engineering from Tel Aviv University and an MBA degree (2007) from INSEAD, France. She has been working for several years as a consultant at McKinsey.

Biographies

Irad Ben-Gal is a faculty member in the Department of Industrial Engineering at Tel Aviv University. He holds a B.Sc. (1992) degree from Tel Aviv University, and M.Sc. (1996) and Ph.D. (1998) degrees from Boston University. He is a member of the Institute for Operations Research and Management Sciences (INFORMS), the Institute of Industrial Engineers (IIE), The European Network for Business and Industrial Statistics (ENBIS) and an elected member in the International Statistical Institute (ISI). He is a Department Editor for *IIE Transactions on Quality and Reliability* and serves on the Editorial Boards of *Trends in Applied Sciences Research* and *The Open Applied Informatics Journal*. He has published more than 60 scientific papers and received several best papers awards. His papers have been published in *IIE Transactions*, *International Journal of Production Research*, *Technometrics*, *IEEE Transactions on Reliability*, *Journal*

Yossi Bukchin is a faculty member in the Department of Industrial Engineering at Tel Aviv University. He received his B.Sc., M.Sc. and D.Sc. degrees in Industrial Engineering and Management from the Technion Israel Institute of Technology. He is a member of the Institute of Industrial Engineering (IIE) and the College-Industry Council on Material Handling Education (CICMHE) and on the Editorial Board of *IIE Transactions*. He has held a visiting position in the Grado Department of Industrial & Systems Engineering at Virginia Tech. His papers have been published in *IIE Transactions*, *Operation Research*, *M&SOM*, *European Journal of Operational Research*, *International Journal of Production Research*, *Annals of the CIRP* and other journals. His main research interests are in the areas of assembly systems design, assembly line balancing, facility design, operational scheduling, multi-objective optimization as well as work station design with respect to cognitive and physical aspects of the human operator.